Sensors and Actuators A 212 (2014) 1–11

Contents lists available at ScienceDirect

Sensors and Actuators A: Physical

journal homepage: www.elsevier.com/locate/sna

Underwater current leakage between encapsulated NiChrome tracks: Implications for strain-gauges and other implantable devices☆

A. Vanhoestenberghe[a,b,*], S. Bickerton[a], S.J.G. Taylor[a], N. de N. Donaldson[b]

[a] Institute of Orthopaedics and Musculoskeletal Science, UCL, RNOH Trust, Stanmore, UK
[b] Implanted Devices Group, Department of Medical Physics and Bioengineering, UCL, London, UK

ARTICLE INFO

Article history:
Received 20 May 2013
Received in revised form 22 January 2014
Accepted 23 January 2014
Available online 20 March 2014

Keywords:
Intelligent prostheses
Strain-gauges
Silicone rubber encapsulation
Long-term implantation

ABSTRACT

We present the results of experiments aimed at identifying a suitable polymer for the encapsulation of thin-film strain gauges for underwater applications (with a view of using it in an instrumented bone fusion nail). The leakage currents across grooves cut (using a laser) in thin films of NiChrome over borosilicate glass were studied for encapsulated samples, immersed in water at 37 °C. The selected encapsulants were five silicone rubbers (of both medical and engineering grades), produced by Nusil (MED-6015, MED4-4220, MED3-4013, CV14-2500 and EPM-2420) and Elast-Eon™2A, a co-polymer developed by Aortech. The effect of a primer, as well as that of a black dye mixed with the rubber, was also investigated.

13% of samples exhibited slow current increases, peaking at 1–4 nA, and 9% exhibited brief peaks up to 30 nA (only one sample exhibited both). These were due to corrosion of the NiCr following ionic contamination. For the remaining 80%, the leakage current remained remarkably low (<1 nA).

Silicone rubber encapsulation appears as a realistic low-cost alternative to the hermetic packaging of thin-film strain-gauges. However, this is conditional to achieving a suitable degree of cleanliness of all surfaces prior to encapsulation. Cleaning and rinsing procedures should therefore be evaluated before opting for this method.

1. Introduction

Silicone rubber encapsulation has been used for many years as a reliable method to prevent moisture damage in electronics operating in high moisture environments [1,2]. One extreme example of this is found in the field of medical engineering, where small electronic devices thus protected are routinely implanted in the human body [3–5]. For some applications, these should ideally remain safe and functional for over 50 years surrounded by body fluids. To offer effective protection, the encapsulation relies on a complete absence of voids over the substrate, not only directly after encapsulation, but for the life of the implant. The rubber shrinks during cure, introducing interfacial stresses that may exceed the adhesive strength of the encapsulant. Voids may then appear while the device is in use, leading to changes in the conductivity between encapsulated tracks. Not only will this eventually result in corrosion damage, it may affect the functional integrity of the circuit over a much shorter period. In applications such as strain measurement, the presence of even very small leakage currents can give erroneous data. The efficacy of silicone rubber encapsulation for long-term human implantation was established several decades ago [6] but with technological advances, many device feature sizes are decreasing. The distance between conductors on thin-film profiles can be less than 10 μm, increasing the electric field strength, possibly decreasing the encapsulated device's lifetime [7]. It also requires the encapsulant to conform to the finer surface topology to prevent corrosion and we do not know how well uncured silicone rubber flows in such narrow grooves.

We are particularly interested in the use of thin-film strain-gauges sputtered onto orthopaedic implant substrates. They offer certain advantages such as long term stability, high gauge resistance and custom-designed layout [8]. This type of gauge was used, albeit hermetically sealed in a dry cavity, in an in vivo study of force measurements in femoral implants [9]. However, a leakage current, shunting the gauge, will cause errors in the apparent strain measurements. Strain gauges with a high impedance are desirable to keep the current consumption down, but this makes them more susceptible to leakage currents. In Section 5 we discuss a typical

* Corresponding author. Tel.: +44 2076790296.
E-mail address: a.vanhoest@ucl.ac.uk (A. Vanhoestenberghe).

0924-4247/$ – see front matter © 2014 The Authors. Published by Elsevier B.V. All rights reserved.
http://dx.doi.org/10.1016/j.sna.2014.01.034

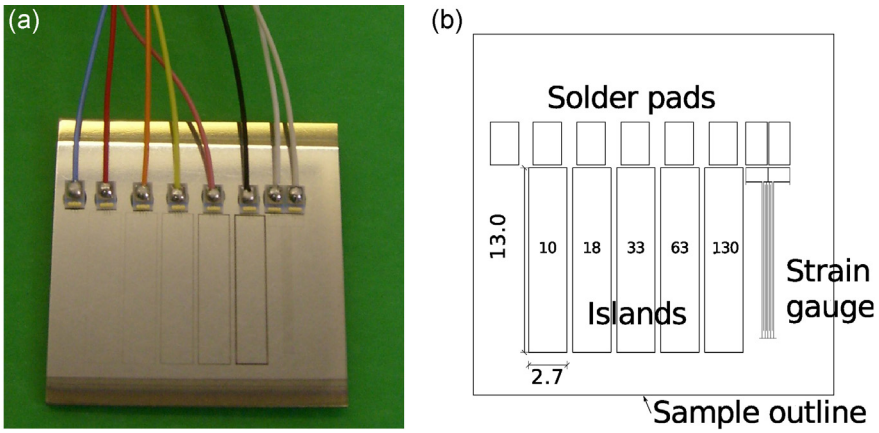

Fig. 1. Test sample. (a) A test piece ready for encapsulation. The blue wire (leftmost) is connected to the substrate, the following five (red, orange, yellow, pink and black) are to the five islands, and the pair of white wires is for the test strain-gauge. (b) Schematic drawing of a sample showing the connection pads, five NiChrome islands and the strain gauge. The number in each island is the width of its insulating groove (μm), the larger numbers are the island dimensions (mm). (For interpretation of the references to color in this legend, the reader is referred to the web version of the article.)

gauge geometry, showing that a current as small as 50 nA could result in an error on the measured strain of 200 με[1]. To compare with measured strains, Al Nazer et al. [10] report strains on the tibia, while walking, as low as 237 με.

In this paper, we report on a study of the underwater leakage performances of NiChrome over borosilicate thin-film test samples prepared as for standard thin-film strain-gauges. For the purpose of these tests, the pieces have various insulator widths and are encapsulated with a range of polymers. Our leakage current recordings evaluate their suitability as encapsulants for strain-gauge applications.

2. Method

2.1. Thin-film structures

To measure only the leakage current across the insulating groove in the NiChrome metallisation, the study was not performed using actual strain-gauges. Instead, insulated "islands" were designed (see Fig. 1) where the only current that could flow is a leakage current. Their dimensions were chosen so that, assuming a purely ohmic response, the currents recorded are about 100 times larger than those expected in a typical orthopaedic thin-film strain-gauge topography, to amplify the effect for the experiment. The test pieces were prepared using typical thin-film strain-gauge materials and methods. Square titanium substrates, 25 mm × 25 mm × 1 mm, were polished, using aluminium oxide and liquid diamond compounds, as required to achieve a surface roughness less than 3 μm. A 5 μm borosilicate layer was sputtered onto the substrates, followed by a 0.25 μm layer of NiChrome resistor alloy. On each substrate, five rectangles were laser-cut[2] in the NiChrome, exposing the glass insulator underneath. All five have the same dimensions (13 mm × 2.7 mm) but the nominal width of the insulating groove cut by the laser is different in each case (10, 18, 33, 63 and 130 μm, depending on the number of passes of the beam, see Fig. 1(b)). The edges cut by the laser however are somewhat irregular, with NiChrome obstructing up to one-third of the gap, and with apparent debris left in the groove (see Fig. 2). Connection pads, approximately 0.25 mm thick with a metallised top layer (with a large silver-palladium area for soldering, and a small gold area for wire bonding), were glued using Ablebond 77-1S non-conductive glue above each rectangle, plus one for grounding the surrounding conductor. Three aluminium wire-bonds join each pad to its respective "island" or to the surrounding metal. A standard strain-gauge structure was also laser-cut onto the substrate (gap width: 10 μm), with two associated connection pads. There are a total of eight pads on each sample, connected to the substrate, the five islands (of equal dimensions but separated from the surrounding conductor with gaps of different width), and the last pair to the test strain-gauge (see Fig. 1(a)).

2.2. Cleaning and encapsulation

After soldering wires to the pads, the samples were immersed in solvent, HFE-72DA (3M), to dissolve both organic and ionic contaminants. The samples were then dried by allowing the solvent to run off into absorbent paper before they were rinsed in flowing de-ionised water and dried in air, at 80 °C. This cleaning method was selected for its simplicity and low cost. It is suitable for a wide range of applications and could easily be scaled up for manufacture [11].

Unless otherwise stated, the rinsing process was continued until the purity of the rinse water reached 7 MΩ cm. The influence of this water's purity was further evaluated in a parallel experiment. Four samples were only rinsed for 20 minutes in re-circulated, store-bought, de-ionised water whose resistivity was measured as lower than 250 kΩ cm. These samples are referred to as "not clean" in the paper, and the results are specifically discussed in Section 4.2.

The tests were designed to study the performance of a range of encapsulants as well as the effect of priming the substrate, and that of mixing a dye with the uncured polymer. The dye tests are relevant to applications using bare semiconductor dice, where dyed encapsulants are used as shields from light which might otherwise affect the integrated circuit (IC)'s function. Table 1 lists the different materials tested, and whether a dye or primer was used. MED-6015, MED4-4220 and MED3-4013 are medical grade silicone rubbers, CV14-2500 and EPM-2420 are engineering grade rubbers,[3] while

[1] A strain is a ratio of forces, and as such dimensionless. However, the Greek letter ε is commonly used to indicate that the number given is a strain, especially when working with multiplying suffixes such as μ. It is more convenient to work with microstrain rather than strain since these levels of strain are more physiological.

[2] The grooves were cut using a lamp pumped, Q-Switched Nd:YAG laser with a 1064 nm wavelength.

[3] Although the engineering grade silicone rubbers are not sold for implantable applications, they were included in our tests for comparison with the three other, medical grade, silicone rubbers. CV14-2500 was considered because it was

Table 1
List of silicone rubber tested and their recommended applications. M: 3 days baseline recordings in air followed by immersion for 1 period of 6 days; L: long test: 3 days baseline followed by two 6 days biased periods separated by a rest of 9 weeks immersed but un-biased; S: shorter test, with 1 hour baseline followed by immersion for 6 days. An extra "b" indicates that the primer was applied using a paint brush (a spray gun was used for all other primed substrates).

Product name	Manufacturer's recommended applications	Alone	Dye	Primer	Dye and primer
MED-6015	Moulding, potting and encapsulating	L	L	L	L
MED-6015 NC[a]		S	S	S, b	S, b
MED4-4220	Protection of electronics	S	L	S, b	L
MED3-4013	Medical adhesive for silicones	S	L		
CV14-2500	Protection of electronics from extremes in humidity and heat, in sensitive applications requiring a material with low outgassing and a superior flow	M	M		
EPM-2420	General purpose protection of electronics, optically clear with superior flow	S	M		
E2A	Biomedical polymer designed for long-term implantation	L			

[a] NC: "not clean" samples, where the purity of the rinse water was lower than 250 kΩ cm as described in Section 2.2.

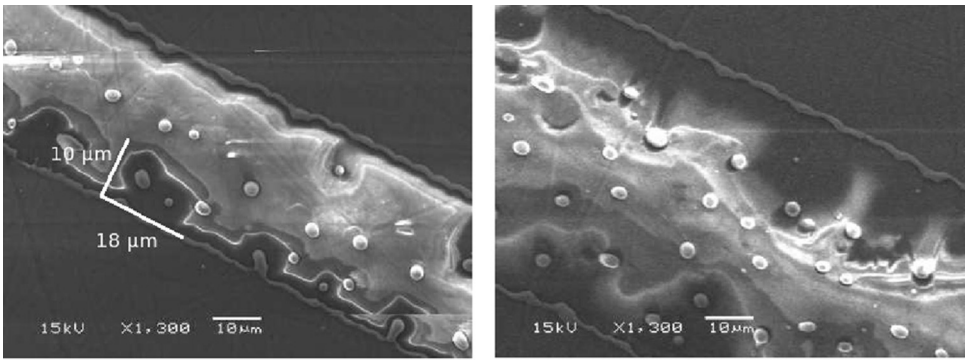

(a) A 33 μm gap. (b) A 63 μm gap.

Fig. 2. SEM photographs of the gaps cut through the NiChrome, showing debris left in the grooves, and possible irregularities along the edges with dimension lines.

Elast-Eon™2A (E2A) is a 2-part biomedical polyurethane produced by Aortech PLC. for long-term implantation. Apart from the E2A, all the silicone rubbers (medical and engineering grades) as well as the primer and dye are produced by Nusil.

The recommended primer, MED6-161, was applied over the clean substrate using either a fine paint brush (indicated by the letter "b" in Table 1) or a spray gun, and left to dry at room temperature (around 21 °C) for 45 minutes. The encapsulants used are 2-part silicones, that were mixed[4] just before use. When used, the dye, MED-4900-2, was added to a ratio of 2% of the volume of the mix.

All test samples were placed in individual trays, filled with the selected encapsulant to cover the surface of the substrate with a layer of approximately 2 mm thickness, then cured in a pressure oven at 70 °C, 2 bar, for 24 h. This thickness may be used to calculate an order of magnitude for the time taken for the silicone rubber to become saturated with water molecules after immersion, using the formula introduced by Fedors [12].

$$t_{\mathrm{eq,min}} = \frac{\pi}{4 * D} * \left(\frac{V}{A}\right)^2 \quad (1)$$

In this equation V is the volume of silicone rubber and A the surface area in contact with liquid water. Their ratio is the rubber thickness ~2 mm. The diffusion coefficient, D, will vary depending on the filler used in the silicone rubber. In Watson and Baron [13], $D = 2 \times 10^{-9}$ m^2/s, which gives an approximative value of the time to equilibrium for the samples used for this experiment of less than an hour.

developed specifically for adhesion to metal and EPM-2420 because it includes an adhesion promoter, has a low curing temperature and low viscosity.

[4] All mixing was done in a Speedmixer™ DAC 150 from Synergy Devices Ltd.

2.3. Set-up and experiment procedure

Wires from each sample were led to an instrumentation box containing Wheatstone bridges, AD621 instrumentation amplifiers and ADC included within an XE88L01A microcontroller. Fig. 3 is a schematic of the circuit inside the enclosure. Arrows indicate where the test structures (nominally open circuit) are mounted in parallel with 20 kΩ resistors (R_b in Fig. 3). These form the lower part of half a Wheatstone bridge, where the upper quarter bridge resistor, R_a, is also 20 kΩ. In groups of three, the half-bridges are connected to a common half-bridge, made of two precision 10 kΩ resistors (R_p). There are four such groups in the box, and multiplexors are used to interrogate each of the half-bridge outputs in turn. Twelve

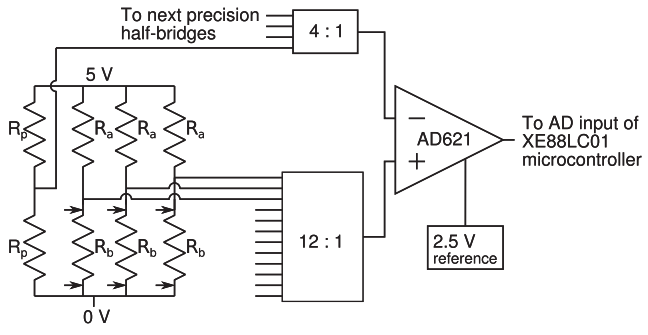

Fig. 3. Schematic of the measurement setup showing only one-fourth of the Wheatstone bridges resistors, and associated data acquisition electronics. The three pairs of arrows indicate where the islands under test are connected (in parallel with R_b). One half of the bridge is formed by two 10 kΩ precision resistors (R_p). For each precision half-bridge there are three corresponding "test" half bridges, formed by R_a = 20 kΩ in series with R_b = 20 kΩ unless a strain-gauge structure is connected (instead of R_b in parallel with an island) in which case R_a is individually adjusted.

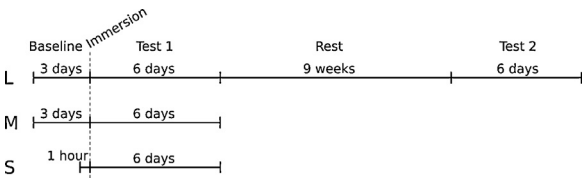

Fig. 4. Duration of the different stages of the experiment for the 3 types, L, M and S.

structures (two groups of five islands plus one strain-gauge each) were therefore tested together, with all bridges continuously biased with a constant 5 V (2.5 V across each test structure). Accurate control of this 5 V bias voltage was unnecessary since dedicated sensing inputs of the XE8801A microcontroller enabled ratiometric measurements of the ADC inputs (specific circuit not shown in Fig. 3). The leakage current through a test structure is calculated as $-2 \times V_{mes}/R_b$, where V_{mes} is the measured voltage. Each channel was sampled at 100 Hz. An average of 16 samples was taken every 5 seconds and this reading was then automatically stored (on the computer controlling the experiment, using Labview 2009) for later analysis. The precision of the system allows us to detect a leakage current with a resolution of −15 pA[5] per step of the ADC (hereafter referred to as "count"). A thermistor monitors the sample's temperature, with readings taken and stored at the same time.

The samples were first biased in air (in the lab, temperature and humidity not controlled) to obtain baseline readings. This first period lasted either 1 hour (label S for "shorter test" in Table 1) or 3 days (for medium (M) and long (L) tests). The samples were then immersed, without interrupting the bias, in water at 37 °C. The thermistor was placed in a small oil-filled container inside the water bath. This first immersion period lasted 6 days, after which some samples were then left for a period of 9 weeks, immersed but unbiased, before a second continuous bias period of 3 or more days. The length of the first bias period was chosen to reflect the full life of a gauge mounted on an orthopaedic prosthesis to monitor bone healing: about 14 months with a daily use of 20 minutes, i.e. 8,500 minutes or 6 days of continuous bias.

The second bias period and the 9 weeks during which the samples remained immersed but unbiased, enabled a distinction to be made between the influence of the bias and that of the immersion duration. (Fig. 4)

2.4. Analysing and plotting the data

The recordings were analysed and plotted using Matlab. The readings were stored as numbers in counts and conversion factors were applied to obtain time, current and temperature values before plotting the data. Only in Fig. 5, the amplitude of the fluctuations about the average was large so a smoothing window was used to reduce the blur, as mentioned in the caption. Whenever present, the right-hand side *y*-axis shows temperature values in °C.

As explained in Section 2.3, the tests all began with baseline readings, with the samples biased, in air, for a duration of 1 hour or 3 days. The samples were then immersed for 6 days without interrupting the bias. Some samples were then left in the water bath for 9 weeks before a second bias period (Table 1). Fig. 5 is a plot of the results of a long test, for clarity, the transition from one period to the next is indicated on the plot by a horizontal gap with a red dotted vertical line.

[5] The "−" sign introduced here accounts for the inverse relationship between the leakage current and the voltage at the Wheatstone bridge's output.

Table 2
Summary of observations. P indicates that a blunt peak was observed (as in Fig. 5(b)), B for rapid current bursts (Fig. 7), T for strong effect of the temperature, V for step changes in the response attributed to variation in the bias voltage and X for nothing noticeable.

Product name	Alone	Dye	Primer	Dye and primer
MED-6015	B	X	P	X
MED-6015 not clean	B	V	P, B	P, B
MED4-4220	T	T	T	T
MED3-4013	T, V	X		
EPM-2420	T	B		
CV14-2500	B	X		
E2A	V			

2.5. Relative current variation

For each sample, the average value of the baseline readings is used as an arbitrary zero. From there, any increase in the current flowing through the load is plotted as a positive current, and a decrease as a negative current. It is important for the interpretation of the plots to stress that the sign of the current along the *y*-axis is not an indication of its direction, but only whether more (for a positive value) or less (negative value) current leaks across the gap after immersion, compared with the average of the baseline readings.

3. Results

3.1. General observations

A total of 95 islands were tested. A summary of the observations is presented in Table 2. They fall in one of the following three categories.

- The current increases during the first few hours after immersion, reaches a blunt peak then returns to close to the baseline level more slowly than it increased. This is labelled "P" in Table 2. It was seen in two of the four short MED-6015 "not clean" sets: those with primer, with and without dye (Fig. 6(b)). The leakage current reached a maximum of about 4 nA in 10 hours. A similar slow increase, reaching lower values (max 1.3 nA at peak), is also present in the results of one set of MED-6015 on a clean substrate, prepared with primer, see Fig. 5(b). All sets included, blunt peaks were observed in a total of 12 islands, or 13% of the test.
- Large, sudden, current increases (by a factor of 10–100) are present. In some cases the current remains relatively high after the initial sharp rise. This was the case with CV14-2500 (10, 18 and 33 μm gap) and EPM-2420 with dye (for the 33 μm gap only), see Fig. 7. In other cases, the duration of the burst is limited and the current returns exponentially towards to its pre-spike level after several hours, as seen again in Fig. 6 for three of the four MED-6015 "not clean" sets: with dye (33 μm gap), with primer (10 μm gap), and with dye and primer (10 and 18 μm gap). These rapid current bursts (B in Table 2) were observed in a total of nine out of 95 islands, or 9% of the test.
- All other cases, or 80% of the samples. The current remains below ±1 nA with fluctuations of up to ±0.5 nA. At these levels, the high-frequency fluctuations render the observations imprecise. The traces show no particular trend. Typical examples are shown in Fig. 5(a) (long test) for all but the 10 μm trace (allowing for the temperature influence), and Fig. 6(a) for all but the 33 μm-with-dye trace.

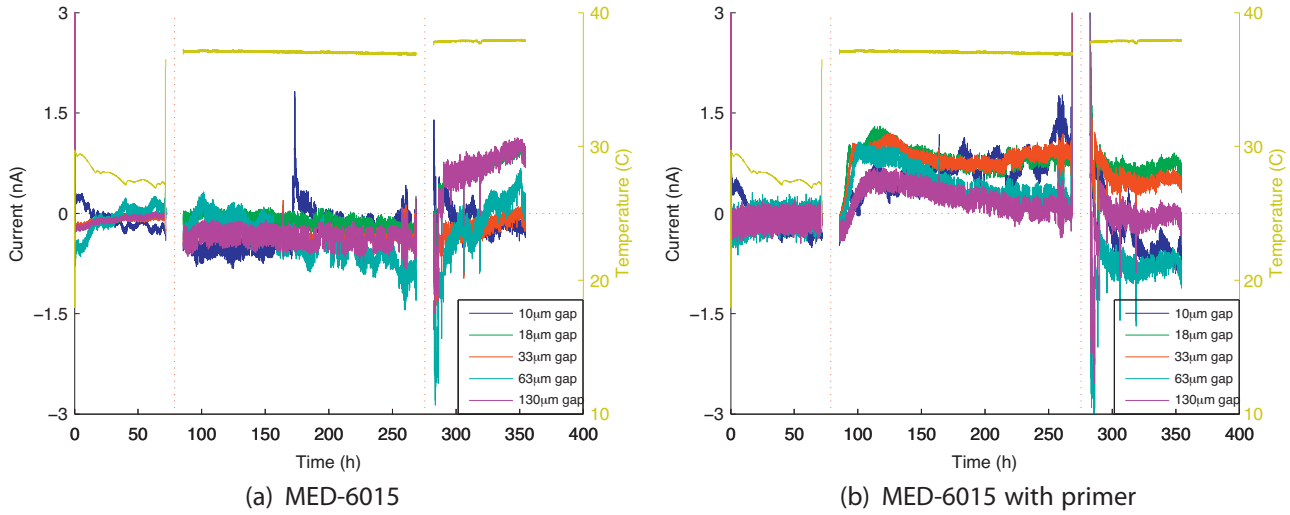

Fig. 5. Current leakage with clean substrates coated with MED-6015 without dye. Baseline period of 3 days (72 hours) followed by two bias periods, the first lasting 7 days (from 90 to 260 hours), the second only 3 days (to 350 hours). Readings were smoothed using a 10-point moving average window. To make the figures easier to interpret, the bias periods are separated by delays of 20 hours that were introduced while plotting and are not a representation of the experimental intervals (no interruption from the baseline to the first immersion period, and 9 weeks between the first and second immersion period).

3.2. Background interferences and influence of the temperature

Despite careful component selection and shielding of the circuit, background interference adds fluctuations of up to ±0.2 nA, visible in Fig. 8. Slower variations are also visible, due to the temperature sensitivity of the recording equipment (mainly the precision resistors forming the Wheatstone bridge), up to 1.5 nA/°C. Some channels are more sensitive than others as seen in Fig. 8.

A calibration test, run without any samples connected to the equipment, shows a high correlation between the temperature and five of the 12 recording channels: $R^2 = 0.75$ on channel 1 (+0.2 nA/°C), $R^2 = 0.96$ on channel 4 (−0.3 nA/°C), $R^2 = 0.85$ on channel 6 (+1.4 nA/°C), $R^2 = 0.98$ on channel 7 (+0.4 nA/°C) and $R^2 = 0.97$ on channel 12 (−1.5 nA/°C). As two sets are under test at any one time, these channel numbers correspond to gaps of 10 μm and 63 μm and the strain gauge in the first set, and the 10 μm gap and strain-gauge in the second set, respectively. For example, the two sets of Fig. 5 were under test together. During the baseline period, the temperature recorded is that of the room, hence the correlation with the current readings can be assessed graphically. The results for the first sets are in Fig. 5(a), the fluctuations of the blue and cyan curves (10 and 63 μm gap) during the baseline period clearly follow those of the temperature. R^2 values were computed between the recorded room temperature and current readings during the baseline periods of all the experiments. Although the actual values vary from one experiment to the next, a good correlation with the same five channels was observed.

3.3. Visual examination of a substrate after the end of the experiment

The "not clean", primed, substrate encapsulated with MED-6015 mixed with dye (results in Fig. 6(b)), was later stripped of its coating for visual inspection. Fig. 9 includes a picture of the sample, and two SEM photographs of damaged areas. The silicone rubber stripping

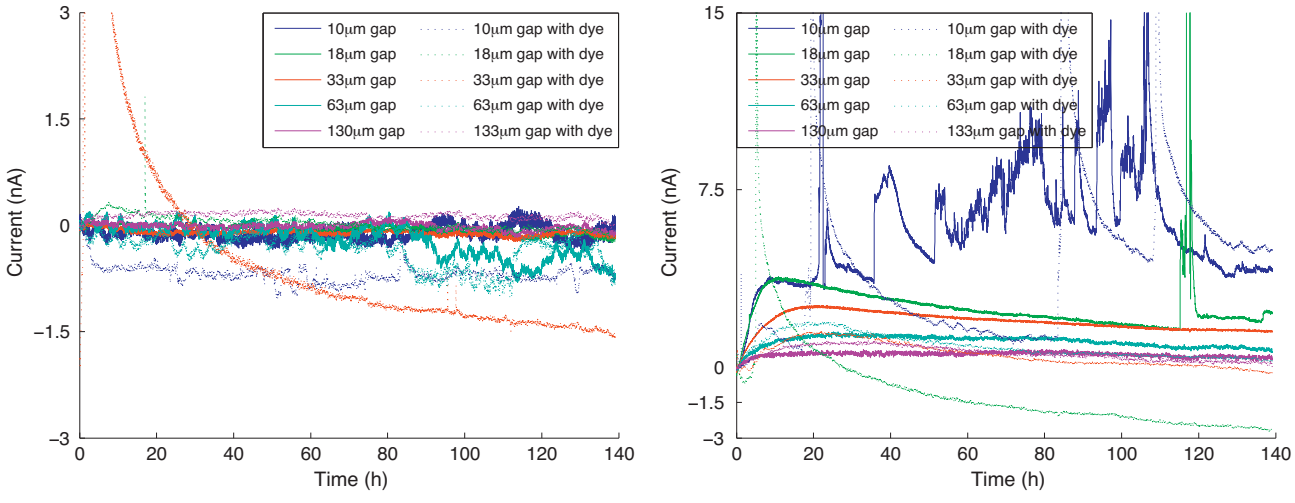

Fig. 6. Current leakage with "not clean" substrates coated with MED-6015. Baseline period of 1 hour followed by a single immersion period of 6 days.

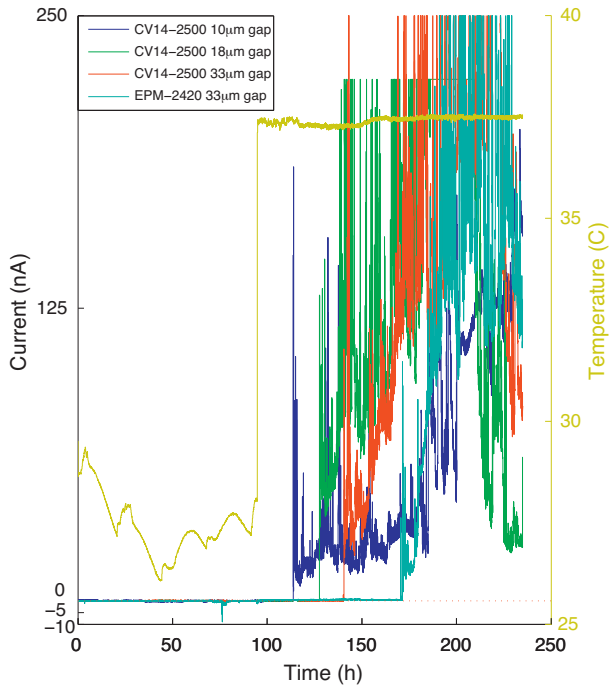

Fig. 7. Rapid bursts and large increases of the leakage current recorded with unprimed substrates coated with CV14-2500 (no dye) or EPM-2420 with dye. Only the channels that exhibited these peaks are plotted, all other gap widths showed no particular trend. The baseline period lasted 4 days (to 95 hours). This is followed by a single bias period of 6 days or 160 hours. For all traces, the current before the peaks was below 1 nA.

process is not known to cause damage to thin-film, hence these brown areas are most probably caused by the corrosive process described in the following discussion (Section 4.2).

4. Discussion

4.1. Artefacts, including influence of the temperature

The recording equipment introduced two known artefacts: fluctuations following the temperature of the room where the circuit was located (see Fig. 8), and electromagnetically induced voltage spikes.

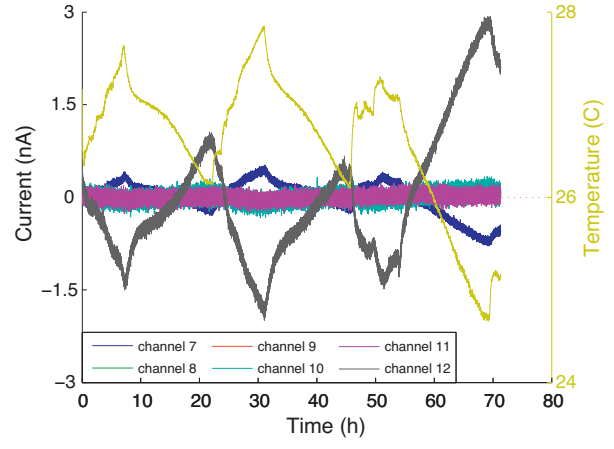

Fig. 8. Apparent current fluctuations recorded without test samples connected, showing the background interferences and influence of the equipment temperature. Only channels 7–12 are plotted here for clarity, the first six channels had similar traces.

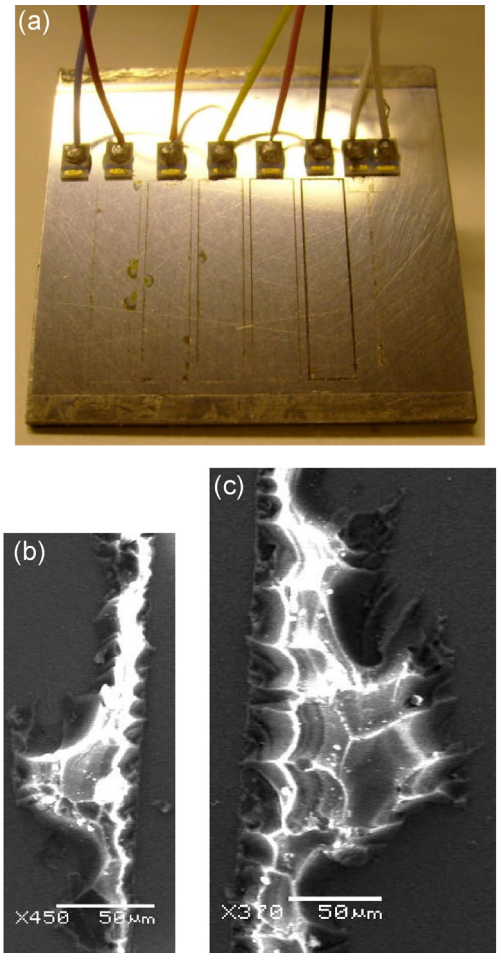

Fig. 9. Damage observed on a sample exhibiting large current spikes with and without partial recovery (see Fig. 6(b)). (a) Photo of the "not clean" sample that had been primed and coated with MED-6015 with dye, after removing the silicone rubber at the end of the test. Brown areas, probably indicating destruction of the thin-film material, are visible in the first three islands. (b) SEM picture of a damage over a 10 μm gap. (c) SEM picture of a damage over a 18 μm gap.

Artefacts due to the latter appear as sharp spikes synchronously present on several traces recorded together. The spikes seen at about 310 and 330 hours on the traces of Fig. 5(a) are also visible on several traces of Fig. 5(b). These samples, clean substrates, primed and unprimed, coated with MED-6015 without dye, were under test together. These artefacts are limited in time and can be visually assessed and disregarded. When the mains power supply was interrupted for a longer time, the bath temperature also dropped (seen at 330 hours).

Likewise, although the ambient temperature can introduce fluctuations of up to ±1.5 nA/°C on the most sensitive channels used for the leakage current recordings (due to the temperature sensitivity of the balance resistors in the bridge), the variations display a 24 hour cyclic pattern as the ambient cools at night and warms up during the day. This is clearly visible in Fig. 8. As the recordings took place over several months, this effect is more pronounced for some sets than others, yet it remains easily identifiable in all cases when it is prominent enough to affect the data. The average room temperature can also fluctuate over several days: see for example the temperature recording during the baseline period of Fig. 5(a). The diurnal cycle is superimposed on a marked downward trend, losing 2.5°C over 3 days, corresponding to an error of 0.5 and −0.8 nA on the current readings of the 10 and 63 μm gaps respectively. It is likely, although we have no ambient temperature data to verify

it, that the ambient temperature started increasing later, leading to the apparent decrease in leakage current visible for the 63 μm gap (Fig. 5(a)). Although less obvious to identify than the power supply glitches, this effect equally affects the five most responsive channels. Hence, the significance of a slow trend seen on any of these could be evaluated by comparing it with the readings from the other temperature sensitive channels.

Glitches and temperature related fluctuations have therefore intentionally been left out of the discussion that follows. Further, with respect to variations in the test water temperature, any bulk strain changes in the polymer would have minimal effect on the strain in the thin-film gauge, since there is a disparity in the moduli of the polymers and the titanium of around 5 parts in 10^6. This is less than the native temperature coefficient of expansion of titanium. Thus this is not a concern for in vivo applications.

4.2. Bursts, blunt peaks and purity of the rinse water

4.2.1. Rapid current bursts

Bursts of current were observed in three of the four "not clean" sets coated with MED-6015, as well as with CV14-2500 (no dye) and EPM-2420 with dye (Fig. 7). In all the sets where these were observed, only the narrowest gaps were affected. None of the clean MED-6015 samples show such bursts, hence we can disregard MED-6015 as being the cause. As summarised in Table 2, they are visible, for at least one gap width, in one-third of all the primed substrates, and one-third of the samples with dye. However, assuming the cause of the bursts in the "not clean" sets is ionic contamination, and excluding them from the tally, these ratios fall to zero primed substrates, one in six with neither dye nor primer and only one in seven when dye was added to the encapsulant. Therefore, the use of either the dye or primer can not be linked to the occurrence of the phenomenon.

We hypothesise that dendrite growth followed by corrosion of the NiChrome metallisation, after the dendrite has bridged the gap, caused these bursts. Fig. 9 shows photographs of the sample that had been primed and coated with MED-6015 with dye, after the end of the experiment (and removal of the coating). Two of the damaged areas (brown in Fig. 9(a)) were further imaged with a SEM (Fig. 9(b) and (c)). At higher magnification, corrosion of the NiChrome is clearly visible. From Figs. 9(c), we estimate that a volume of NiChrome of the order of 10^{-9} cm^3 has been dissolved. With a specific gravity of the NiChrome ≈8.4 g/cm^3, this gives a mass of the order of 10^{-8} g. Using Faraday's law of electrolysis (Eq. (2)), this corresponds to a charge of the order of 10^{-5} C.

$$Q = z \times F \times \frac{m}{M} \tag{2}$$

$$\begin{aligned} \text{with the valency } z &= 2 \\ \text{the Faraday constant } F &= 96,485 \ \ \text{C/mol} \\ \text{and the molar mass of NiChrome } M &= 260\,\text{g/mol} \end{aligned} \tag{2}$$

This can be compared to the charge corresponding to the area under the first peak of the 10 μm gap of the "not clean" primed substrate coated with dyed MED-6015 (see Fig. 6(b)). Using Eq. (3), we estimate the latter as 6×10^{-6} C. The two charges are in the same order of magnitude, supporting our hypothesis that the current burst is due to the NiChrome corrosion.

$$Q = \int_0^T I_{\text{peak}} \times e^{-t/\tau} dt \tag{3}$$

$$= I_0 \times (-\tau) \times [e^{-t/\tau}]_0^T \tag{4}$$

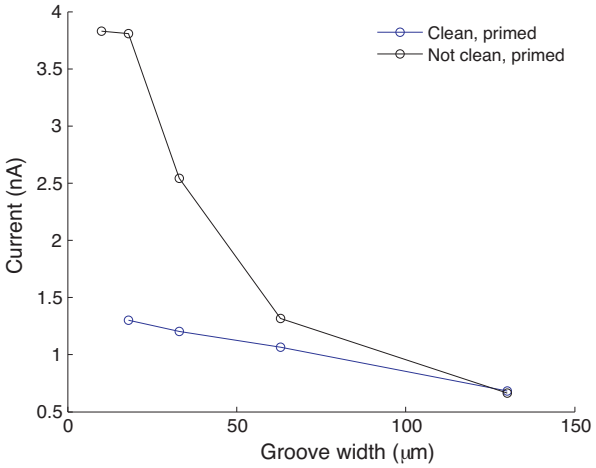

Fig. 10. Maximum current level reached at the top of the blunt peak that follows immersion, versus groove width, for two sets: clean and unclean substrates, both primed and coated with MED-6015. The results of the tests are plotted in Figs. 5(b) and 6(b) respectively.

$$\begin{aligned} \text{with the peak current } I_0 &\approx 10 \ \ nA \\ \text{the time constant } \tau &\approx 600 \ \ \text{s} \\ \text{and } T \gg \tau \rightarrow [e^{-t/\tau}]_0^T &\approx 1 \end{aligned} \tag{4}$$

In Fig. 6(b), the current presents a sharp initial increase, which is clearly followed by an exponential recovery for the dyed encapsulant. In Fig. 7 however, the level fluctuates noisily as the first rise is followed by several others in quick succession. Hence the current remains high for some time before initiating a partial recovery. For all samples affected, only the narrower gaps show such sudden increases, with complete or partial recovery. Further experiments are needed to better understand the recovery period, and whether it always occurs or not.

4.2.2. Cleanliness

The "not clean" samples were rinsed using low purity de-ionised water bought in a haberdashery store. Its resistivity was lower than 250 kΩ cm, whilst the high-purity water, used for all other samples, has a resistivity of 10 MΩ cm. The results from the un-primed substrates show no slow increases (Fig. 6(a)). There is a spike for the 33 μm gap with dye, about 1 hour after immersion. On the primed substrates, blunt peaks are visible for nearly all gap widths and bursts are present for the 10 and 18 μm gaps (with and without dye).

Of the 15 clean substrates, a blunt peak is only visible for one substrate, primed and coated with MED-6015. Bursts were observed in two sets: CV14-2500, 10, 18 and 33 μm gaps and EPM-2420 with dye, 33 μm gap. Considering the blunt peaks and bursts as "events", our results give event ratios of 20% for clean substrates versus 75% for the "not clean" substrates, highlighting the importance of ionic contamination in the encapsulant insulation failure.

4.2.3. Blunt peaks

Such an increase of the current during the first 10–20 hours after immersion followed by a slower exponential decay, is regularly observed in leakage current studies where it has been attributed to polarisation and depletion of charge carriers [14–17]. It was observed in the two primed "not clean" substrate sets (Fig. 6(a)). The only other set where a similar blunt peak is visible is with the "clean" substrate primed and encapsulated with MED-6015 (Fig. 5(b)). A comparison between the two plots shows a difference in peak values between the "not clean" and "clean" substrates, the leakage for the latter reaching a noticeably lower level (Fig. 10).

Although all three of the samples exhibiting this behaviour were primed, no such peaks were observed for the other three primed samples. Of the six primed substrates, the primer was applied by brush on three, and by spray gun on the other three. A peak is visible on the results obtained with two of the former and one of the latter. No strong conclusion can therefore be drawn as to the influence of either dye or primer, and its application mode, on this phenomenon. Further, the cleanliness of the rinse water alone could account for the blunt peaks as the charge carrier's most likely origin is salt contamination. We propose, in the following paragraph, a possible explanation for this effect, assuming only the presence of ionic contaminants.

As the silicone rubber saturates with water vapour, water may condense at the interface between the encapsulant and the substrate, wherever adhesion has been lost [7]. This forms a small volume of fluid that may stretch across part of the narrow gap. Where present, ionic contaminants turn this film of water into an electrolyte, leading to an initial increase of the leakage current, proportional to the amount of ions available. Although no experiment was performed to verify this, the timing of the observed peaks agrees with the following, gross theoretical estimations. The time taken to fill a volume V with water permeating through a saturated silicone rubber membrane of surface A is:

$$t = \frac{V}{A} * \frac{1}{D * V_m},$$

where $D = 5 * 10^{-5}$ mol/m^2 s [13] and the molar volume of water at 37 °C, $V_m = 1.8 \times 10^{-8}$ m^3/mol. In an area where adhesion between the encapsulant and the borosilicate glass is lost, the water forms a film at the bottom of the groove. If the film is rather flat, the area A through which the water permeates may be taken equal to the surface area occupied by the water, A_s. This approximation no longer holds once the film forms a bubble ($A > A_s$). The film thickness $f_t = V/A_s$, hence, when $A = A_s$,

$$t = 1110 * f_t$$

if f_t is expressed in nm and t in s. In words: it takes about 18 minutes to form a film of 1 nm wherever the adhesion at the bottom of a groove is lost, and this, irrespective of how much of the area of the groove becomes occupied by this film of water.

As the applied bias is constant (5 V), the leakage current (i_L) across the gap then depends on the conductivity of the electrolyte formed by the water as it condenses in the groove (previously contaminated by the low purity rinse water), and its dimensions: gap width (g_w), film thickness and film length (f_l).

$$\begin{aligned} i_L &= \frac{V}{R} \\ \text{where the resistance } R &= \rho \times \frac{g_w}{f_t \times f_l} \\ \text{Re-writing to express the resistivity } \rho &= V \times \frac{1}{i_L \times g_w} \times f_l \times f_t \end{aligned} \quad (5)$$

To illustrate the importance of contamination, let us take two examples from our measurements: 4 nA across a $g_w = 10$ μm ($i_L \times g_w = 40$ pA cm) and 2.5 nA with a $g_w = 33$ μm ($i_L \times g_w = 82.5$ pA cm). Fig. 11 is a plot of the resistivity calculated using Eq. (5) as a function of the film thickness. The film length is given as the fraction of the island perimeter (3.1 cm in total) along which the water bridges the gap. This figure shows that for a current of 4 nA to flow across a 10 μm gap 10 hours after immersion (i.e. when the film thickness is 33 nm), as observed in Fig. 6(b), the resistivity must be 65 kΩ cm if the electrolyte occupies 1% of the perimeter (see the black dotted lines in Fig. 11). Assuming the contaminant is sodium chloride, this corresponds to 7.5×10^{-16} g of NaCl dissolved in the volume

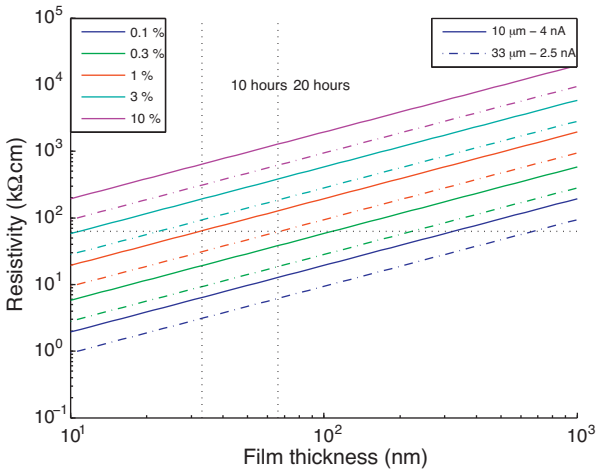

Fig. 11. Resistivity (Eq. (5)) of the electrolyte needed for a given current (4 or 2.5 nA) to flow across a given gap width (10 or 33 μm) as a function of the liquid film thickness when the loss of adhesion, expressed as a fraction of the perimeter, is 0.1, 0.3, 1, 3 or 10%.

of condensed water. Over a similar surface area, rinse water with a conductivity of 250 kΩ cm could leave up to 1.5×10^{-15} g of NaCl after evaporation. For a similar resistivity to lead to a leakage current of 2.5 nA after about 20 hours across a 33 μm gap (again, see results plotted in Fig. 6(b)), only 0.1% of the perimeter would be bridged by the electrolyte. An equivalent loss of adhesion for a clean substrate, where the conductivity of the water in the pocket, in the absence of any external ionic contamination, can be as high as 15–18 MΩ cm, would lead to a leakage current between 14 and 17 pA after 10 hours across a 10 μm gap and about 10 pA for the 33 μm gap after 20 hours (smaller than the fluctuations of the recorded signal).

These calculations, although purely theoretical, support the suggestion that ionic contamination alone, due in our case to a less stringent rinsing process, is responsible for the blunt peaks seen in Fig. 6(b).

Within all plotted sets reaching a blunt peak, the maximum value tends to be smaller for larger gap widths, see Fig. 10. Although unlikely, let us for the sake of argument assume a homogeneous contamination, in terms of salt particles per unit area. At any given point in time, the electrolyte conductivity should then be equal for all the islands. An increase of the groove's width should lead to an equivalent increase in the impedance between the edges of the groove, hence there should be an inverse linear relationship between the gap width and the leakage current level. However, the peaks are not all reached after the same time immersed, and the amplitude of the leakage current does not solely depend on the initial contamination level. Other factors, such as the equilibrium between osmotic and encapsulant pressure, will affect the electrolyte conductivity. Hence the deviation from a linear relationship as seen in Fig. 10 where the first two peaks for the "not clean" substrate reach a very similar level.

Several studies on the failure mechanisms of ICs in humid environment report a similar slow decrease of the leakage current between biased interdigitated aluminium combs exposed to high temperature and high relative humidity environments [17–19]. An initial increase, as observed here, was only reported for encapsulated test samples in Iannuzzi [16]. The other sources, report only a slow decrease (after an initially constant plateau for most encapsulated samples), lasting for over 1000 hours, although the rate of change decreases over time. Although it has been known for many years, we have yet to find a complete explanation for this phenomenon. The authors of the quoted papers explain the shape of

the peaks by the slow drift of the ionic charge carriers, induced by the applied bias, followed by reactions at the electrodes forming non-conducting products.

4.3. Influence of silicone rubber, dye and primer

Excluding the "not clean" substrates, a total of 75 "islands" on 15 samples were tested. As summarised in Table 2, bursts of current were observed for two substrates, for the narrowest gaps, and only one substrate showed a blunt peak, for all gap widths. These three failed substrates are: MED-6015 with primer (blunt peaks on all five gap widths, see Fig. 5(b)), CV14-2500 (large bursts for 10, 18 and 33 μm gap widths, see Fig. 7) and EPM-2420 with dye (33 μm gap only, see Fig. 7 again). MED-6015 was tested on four substrates: bare without dye, primed without dye, bare with dye and primed with dye. As a blunt peak was only observed with one of them, this phenomenon cannot be attributed to the silicone rubber used. Two substrates were tested with CV14-2500 and two with EPM-2420, or ten islands for each, giving failure rates of 30 and 10%, respectively.

A possible increased risk could be attributed to combinations such as primer with MED-6015 (for blunt peaks) and dye mixed with CV14-2500 (for sharp surges). However, no such conclusion can be drawn from our limited set of results and further tests would be needed to study these combinations specifically.

None of the five silicone rubbers tested, nor the E2A co-polymer, should therefore be ruled out as encapsulants. Likewise, neither the use of a primer (whether applied by brush or spray gun) nor that of a dye may be associated with an increased failure risk. While it has no demonstrated negative effect, the primer has also been shown to be unnecessary to prevent failure.

4.4. Immersion unbiased

The influence of a period of immersion (9 weeks) without bias was also studied with a subset of six samples. Several factors, such as the different ambient temperature and a slight change in bias voltage, may explain the apparent discontinuity between the readings from one bias period to the next. These differences remain within 2 nA, and there were no current bursts after reconnection.

The decreasing trend initiated before the unbiased period can be observed in the second bias period of the primed substrate coated with MED-6015 (Fig. 5(b)). This is the only clean sample that exhibited a slow current increase followed by an exponential recovery after immersion. Some of the charge carriers that had contributed to the current increase as the voids filled with water after immersion may have become available again during the unbiased immersion period. Upon reconnection, they contribute to the current leakage, which decreases as the charge carriers become once more immobilised, as happened during the exponential return to the lower leakage level after immersion.

No trend was observed for the five other samples. Therefore, provided there is no ionic contamination, an extra immersion period of 9 weeks does not noticeably affect the quality of the encapsulation.

From our data we cannot conclude whether immersion or bias is more likely to cause leakage. If the samples are prepared carefully, neither a continuous bias for 6 days nor an immersion period of 11 weeks causes a significant increase in leakage current.

5. Application to implantable thin-film strain-gauges

Compared to conventional foil gauges, thin-film gauges are thinner, can occupy a smaller surface area with a geometry designed to fit the application, may be dimensioned to have a larger electrical resistance, and do not require the use of an adhesive (which should eliminate creep as one cause of error in the strain measurement).

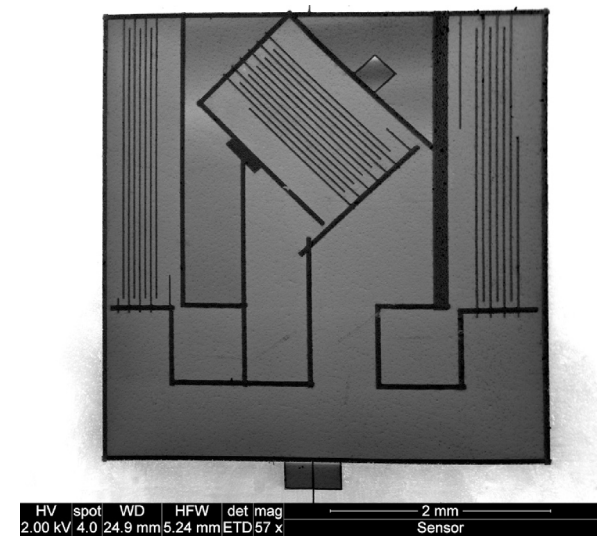

Fig. 12. Field emission electron microscope picture of typical thin-film strain gauges: three in this image. The grooves in the vertical gauges are 2.5 mm long.

Thin film gauges are therefore more suitable for some orthopaedic applications. Implanted gauges are most often protected in a hermetic package to maintain low humidity [20]. However, sufficient hermeticity may be difficult to achieve and the cost and additional volume of this hermetic package may be prohibitive. Low permeability coatings such as commercial insulating resins have been used for short-term strain studies [21]. That choice of material is surprising since decades of studies in the reliability of ICs operating in moist environments have shown the superiority of silicone rubber over epoxy and resins as an encapsulant. Indeed in [21] the authors report a noticeable drift over the 33 hours of recording. Resins should not be considered for underwater operations. Thanks to a combination of good adhesion, high compliance of the silicone rubber and low viscosity uncured, these polymers are a possible alternative to hermetic packaging [7].

In this paper we have tested several encapsulants to evaluate their performance in preventing leakage currents in thin-film strain-gauges. Excluding the surges attributed to ionic contamination, which can be prevented with adequate cleaning prior to encapsulation, the maximum leakage recorded in our study is about 4 nA (blunt peak for "not clean" substrates, see Section 4.2.3). For the clean substrates, the leakage current at peak was below 1.5 nA. In our experiment, the thin-film structures were deliberately dimensioned to exaggerate the leakage effect. The actual current leakage expected in a real gauge, as shown in Fig. 12, mounted as a quarter bridge, would be one-hundredth of this value, or 15 pA.

The change in apparent strain due to a leakage current i_L is

$$\Delta\varepsilon_L = \frac{-R \times i_L \times 2}{S \times V_{\text{bias}}}$$

where R is the quarter bridge resistance, $S = 2.1$ is the gauge factor and V_{bias} is the bias voltage across the Wheatstone bridge. Taking V_{bias} as 5 V and $R = 20\,\text{k}\Omega$ gives an apparent strain $\Delta\varepsilon_L = 3.8 \times 10^{-6}\,\varepsilon/\text{nA}$ or $0.06\,\mu\varepsilon$ for a leakage current of 15 pA (equivalent to the 1.5 nA observed in our test samples). For bone fusion applications, Crawshaw et al. [22] suggest that a drift of the strain measurement $\leq$10% in 24 weeks is acceptable. In a review by Al Nazer et al. [10], tibial strains measured during walking (in several situations) ranged from 237 to 1250 $\mu\varepsilon$. The leakage current we recorded would lead to an error in the strain measurement of 2.5×10^{-4}% of the lowest of these strain values.

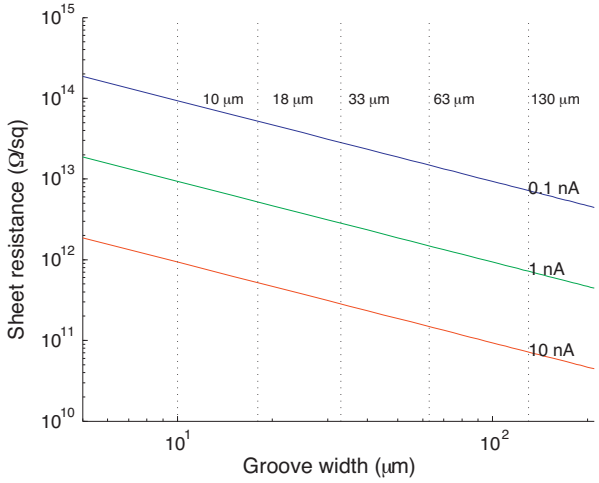

Fig. 13. Sheet resistance as a function of the groove width for several leakage currents levels. The vertical black dotted lines indicate the widths used for our samples.

Consequently, silicone rubber encapsulation could be suitable for implantable strain-gauge applications. There was no drift over 6 days continued bias, and an immersion duration of up to 11 weeks. This indicates that silicone rubber encapsulation would not introduce a considerable error in the strain measurement for a device used (i.e. biased) two hours a day for 11 weeks.

5.1. Sheet resistance

Although these experiments were performed with the strain-gauge application in mind, and hence the results are presented in terms of leakage current, it is also interesting to consider the sheet resistance across the groove. The relation between the sheet resistance (in Ω/sq) and the width of the insulating groove is plotted in Fig. 13 for several values of current. The largest leakage current observed with the blunt peaks, at 4 nA for the 10 μm gap width, corresponds to 2×10^{12} Ω/sq. With currents below 0.5 nA, as was often the case when no trend was observed, the sheet resistance ranges from 10^{13} to 10^{14} Ω/sq depending on the groove width. For comparison, in Davidson and Senturia [23], the sheet resistance of thin-film aluminium oxide (uncoated), in air, at room temperature, ranged from 10^{15} to 10^{12} Ω/sq as the relative humidity increased from 5 to 50%. Data for surfaces coated with silicone rubber are found in Christou and Wilkins [24], with SiO_2 samples coated with either of two Dow Corning silicone rubbers: DC90792 and DC96084. At 23 °C, the sheet resistance ranged from 10^{17} to 10^{13} Ω/sq for both as the relative humidity was increased from 10 to 90% RH. The increase was non-linear, with the rate of change increasing as the relative humidity reached higher values. It is likely that the sheet resistance at 100% RH would have been of the order of 10^{12} Ω/sq. This comparison strongly suggests that, in our experiments, the silicone rubber effectively fills even the narrowest groove (10 μm).

6. Conclusion

One aim of these experiments was to identify a suitable encapsulant for thin-film strain gauges for orthopaedic applications. All of those tested in this study (Nusil MED-6015, MED4-4220, MED3-4013, CV14-2500, EPM-2420 and E2A) performed remarkably well, provided the substrate was thoroughly cleaned before encapsulation. Ionic contamination was identified as the most likely cause of increased leakage current. The use of a dye mixed with the rubber had no effect on the leakage current, nor did the use of a primer. The co-polymer (E2A) has the highest viscosity un-cured, and highest modulus after cure, yet even with this product we observed no unusual events (although, as seen in Table 1, data are only available for one set of islands, as the product was not tested with either a dye or a primer).

Silicone rubber, and possibly co-polymer, encapsulation, thus appears as a realistic low-cost alternative to hermetic packaging of thin-film strain-gauges. However, this is conditional to achieving a suitable degree of cleanliness of all surfaces prior to encapsulation. Cleaning and rinsing procedures should therefore be evaluated before opting for this method.

Competing interests

None declared.

Ethical approval

Not required.

Acknowledgements

The authors wish to acknowledge the financial support of Smith and Nephew and the UK Technology Strategy Board.

References

[1] P.E.K. Donaldson, Twenty years of neurological prosthesis-making, J. Biomed. Eng. 9 (October) (1987) 291–298.
[2] L. Bowman, J.D. Meindl, The packaging of implantable integrated sensors, IEEE Trans. Biomed. Eng. BME-33 (2) (1986) 248–255, http://dx.doi.org/10.1109/TBME.1986.325807.
[3] G.S. Brindley, The first 500 patients with sacral anterior root stimulator implants: general description, Paraplegia 32 (12) (1994) 795–805.
[4] P. Troyk, R. Jaeger, M. Haklin, J. Poyezdala, T. Bajzek, Design and implementation of an implantable goniometer, IEEE Trans. Biomed. Eng. BME-33 (2) (1986) 215–222, http://dx.doi.org/10.1109/TBME.1986.325893.
[5] A. Ramachandran, M. Schuettler, N. Lago, T. Doerge, K.P. Koch, X. Navarro, et al., Design, in vitro and in vivo assessment of a multi-channel sieve electrode with integrated multiplexer, J. Neural Eng. 3 (2) (2006) 114–124, http://dx.doi.org/10.1088/1741-2560/3/2/005.
[6] P.E.K. Donaldson, Hydrothermal stability of joints, using a silicone rubber adhesive, for a range of adherents of interest to makers of surgically-implanted microelectronic devices, Int. J. Adhes. Adhes. 14 (2) (1994) 103–107.
[7] A. Vanhoestenberghe, N. Donaldson, Corrosion of silicon integrated circuits and lifetime predictions in implantable electronic devices, J. Neural Eng. 10 (3) (2013), http://dx.doi.org/10.1088/1741-2560/10/3/031002.
[8] A.J.C. Lee, S.J. Taylor, N. Donaldson, Strain Telemetry in Orthopaedics, Chapman & Hall, 1992, pp. 88–108 (Chapter 6).
[9] S. Taylor, P. Walker, J. Perry, S. Cannon, R. Woledge, The forces in the distal femur and the knee during walking and other activities measured by telemetry, J. Arthroplasty 13 (4) (1998) 428–437.
[10] R. Al Nazer, J. Lanovaz, C. Kawalilak, J. Johnston, S. Kontulainen, Direct in vivo strain measurements in human bone a systematic literature review, J. Biomech. 45 (1) (2012) 27–40.
[11] B.N. Ellis, Cleaning and Contamination of Electronics Components and Assemblies, Electrochemical Publications, Ayr, Scotland, 1986.
[12] R. Fedors, Absorption of liquids by rubber vulcanizates, Polymer 20 (9) (1979) 1087–1090.
[13] J.M. Watson, M.G. Baron, The behaviour of water in poly(dimethylsiloxane), J. Membr. Sci. 110 (1) (1996) 47–57.
[14] S. Sim, R. Lawson, The influence of plastic encapsulants and passivation layers on the corrosion of thin aluminium films subjected to humidity stress, in: 17th IEEE Annual Reliability Physics Symposium, 1979, pp. 103–112.
[15] H. Koelmans, Metallization corrosion in silicon devices by moisture-induced electrolysis, in: 12th Annual Reliability Physics Symposium, 1974, pp. 168–171, http://dx.doi.org/10.1109/IRPS.1974.362643.
[16] M. Iannuzzi, Bias humidity performance and failure mechanisms of nonhermetic aluminum SIC's in an environment contaminated with Cl2, IEEE Trans. Components Hybrids Manuf. Technol. 6 (2) (1983) 191–201.
[17] N.L. Sbar, R.P. Kozakiewicz, New acceleration factors for temperature, humidity, bias testing, in: Proc. 16th Annual Reliability Physics Symposium, 1978, pp. 161–178.
[18] M. Iannuzzi, Reliability and failure mechanisms of nonhermetic aluminum SIC's: literature review and bias humidity performance, IEEE Trans. Components, Hybrids Manuf. Technol. 6 (2) (1983) 181–190.
[19] M. Iannuzzi, Development and evaluation of a preencapsulation cleaning process to improve reliability of HIC's with aluminum metallized chips, IEEE Trans. Components Hybrids Manuf. Technol. 4 (4) (1981) 429–438.

[20] S. Taylor, P. Walker, Forces and moments telemetered from two distal femoral replacements during various activities, J. Biomech. 34 (7) (2001) 839–848.
[21] W. de Jong, J. Koolstra, L. van Ruijven, J. Korfage, G. Langenbach, A fully implantable telemetry system for the long-term measurement of habitual bone strain, J. Biomech. 43 (3) (2010) 587–591.
[22] A.H. Crawshaw, G.W. Hastings, J. Dove, The implanted electrical resistance strain gauge: in vitro studies on data integrity, J. Med. Eng. Technol. 15 (2) (1991) 72–77.
[23] T.M. Davidson, S.D. Senturia, The moisture dependence of the electrical sheet resistance of aluminum oxide thin films with application to integrated moisture sensors, in: Proc. 20th Annual Reliability Physics Symposium, 1982, pp. 249–252.
[24] A. Christou, W. Wilkins, Assessment of silicone encapsulation materials: screening techniques, in: Proc. 15th Annual Reliability Physics Symposium, 1977, pp. 112–119.

Biographies

Anne Vanhoestenberghe received the engineering degree from the Université libre de Bruxelles (ULB), Belgium, in 2001 and the PhD degree from the University of London, UK, in 2007. She is currently a lecturer with the Aspire Centre for Rehabilitation Engineering and Assistive Technology (CREATe), University College London (UCL), UK.

Her research interests focus on the development and packaging of electronic devices for long-term human implantation.

Dr Shixin Bickerton studied at University College London, where she received an iBSc in Orthopaedic Science in 2010 and the MBBS in 2013. She is current an FY1 in General Surgery, Stoke Mandeville Hospital (Buckinghamshire NHS Trust).

Stephen JG Taylor received his BSc in Electrical and Electronic Engineering from the University of Bath in 1979. He worked in electrical instrument development for 2 years before entering the field of medical telemetry. He gained his MSc in Medical Electronics and Physics in 1983 from the University of London. After a further period in industrial instrumentation he became Senior Research Fellow at UCL Institute of Orthopaedics and Musculoskeletal Science, Stanmore. He gained his PhD in 1998 at UCL and is currently a Lecturer in Biomedical Engineering at the Institute of Orthopaedics and Musculoskeletal Science (IOMS), UCL. He has developed several instrumented orthopaedic implants, associated telemetry systems and calibration rigs for measuring dynamic joint forces *in vivo*, and conducted clinical trials to study implant loosening and isometric implant forces. He designed a novel magnetic drive system for the UCL extendible prosthesis for non-invasive bone tumour paediatric limb lengthening, now implanted in several hundred children worldwide. He is Course Tutor for the iBSc in Orthopaedic Science at IOMS. He is co-author of 15 journal articles. His research interests are implantable telemetry for force measurement, fracture healing, in vivo electromyography, implant fixation, and model validation; in vivo measurement for prosthetic control; remote monitoring for wheelchair user accessibility; electronic packaging.

Nick Donaldson studied Engineering and Electrical Sciences at Cambridge University, graduating in 1974. From 1977 to 1992 he worked for the Medical Research Council, Neurological Prostheses Unit, under the direction of Professor G.S. Brindley. In that period, his main field of research was the technology and use of implanted device for the restoration of useful leg function to paraplegics. Since 1992, he has been Head of the Implanted Devices Group at University College London. He has been Principal Investigator for many projects related to implanted devices and functional electrical stimulation. He is a Professor in the University and teaches a course called 'Medical Electronics & Neural Engineering'. His research interests now include implanted device technology, the development of devices that use natural nerve signals as inputs; stimulators of nerve roots in paraplegia; the use of electrical stimulation for recreational exercise of paralysed legs; and methods to encourage functional neurological recovery after injury. He has published over 90 papers in peer-reviewed journals.